Colloid Polym Sci (2008) 286:1411–1423
DOI 10.1007/s00396-008-1912-0

ORIGINAL CONTRIBUTION

Convectional, sedimentation, and drying dissipative patterns of colloidal silica (183 nm in diameter) suspensions in a glass dish and a watch glass

Tsuneo Okubo

Received: 14 June 2008 / Revised: 15 July 2008 / Accepted: 25 July 2008 / Published online: 16 August 2008

Abstract Convectional, sedimentation, and drying dissipative structural patterns formed during the course of drying aqueous colloidal crystals of silica spheres (183 nm in diameter) have been studied in a glass dish and a watch glass. Spoke-like convectional patterns were observed in a watch glass. The *broad ring* sedimentation patterns formed especially in a glass dish within 30–40 min in suspension state by the convectional flow of water and colloidal spheres. The macroscopic broad ring drying patterns formed both in a glass dish and a watch glass. The ratio of the broad ring size in a glass dish against the initial size of suspension, i.e., inner diameter of the glass dish, d_f/d_i, in this work, were compared with previous work of other silica spheres having sizes of 305 and 560 nm and 1.2 μm in diameter. The d_f/d_i values in a glass dish increased as sphere concentration increased, but were rather insensitive to colloidal size. The d_f/d_i values on a watch glass also increased as sphere concentration increased, and further increased as sphere size decreased. Segregation effect by sphere size in a watch glass takes place by the balancing between the upward convectional flow of spheres in the lower layers of the liquid and the downward sedimentation of spheres. Colorful microscopic drying patterns formed both in a glass dish and a watch glass.

T. Okubo (✉)
Institute for Colloidal Organization,
Hatoyama 3-1-112, Uji,
Kyoto 611-0012, Japan
e-mail: okubotsu@ybb.ne.jp

T. Okubo
Cooperative Research Center, Yamagata University,
Johnan 4-3-16,
Yonezawa 992-8510, Japan

Keywords Convectional pattern · Sedimentation pattern · Drying pattern · Colloidal silica spheres · Broad ring pattern · Size segregation · Colloidal crystal

Introduction

Generally speaking, most structural patterns in nature form via self-organization accompanied with the *dissipation* of free energy and in the non-equilibrium state. Among several factors in the free energy dissipation of aqueous colloidal suspensions, evaporation of water molecules at the air–water interface and the gravitational convection are very important. In order to understand the mechanisms of the dissipative self-organization of the simple model systems instead of the much complex nature itself, the authors have studied the *convectional*, *sedimentation*, and *drying* dissipative patterns in the course of dryness of colloidal suspensions as systematically as possible, though the three kinds of patterns are correlated strongly and overlapped to each other.

The most famous *convectional* pattern is the *hexagonal circulating* pattern, *Bernard cell*, and it has been observed when liquids contain plate-like colloidal particles as monitors and were heated homogeneously in a plain pan [1–3]. Another typical convectional dissipative pattern is the spoke-like one and observed in the Bernard cells and also appeared in various substrates sometimes accompanied with the huge number of small *cell convections*. The spoke patterns with cell convections were observed formerly for the membranes of Chinese black ink on water by Terada et al. [4–7], Thus, the author likes to call the spoke-like pattern as *Terada cell*. The convectional patterns, especially Terada cells, were observed directly in the initial course of dryness of Chinese black ink in a glass dish [8], the aqueous and 100% ethanol suspensions of colloidal silica

spheres [9; this work], a cup of Miso soup (Okubo, publication in preparation), coffee [10; Okubo, publication in preparation] or black tea (Okubo, publication in preparation), and colloidal crystals of poly (methyl methacrylate) spheres on a cover glass and a watch glass [11, 12] in our laboratory. Distorted Bernard cells were often observed for Miso soup, coffee, and black tea. For the 100% ethanol suspensions of colloidal silica spheres, Terada cell-type vigorous convectional flow was observed clearly with the naked eye, and the convectional patterns changed dynamically with time. Deegan et al. [10] have reported traces of spoke-like patterns under a microscope. They introduced the capillary flow theory instead of the convectional flow of the liquid from the pinning effect of the contact line of the drying drop. From our series of drying experiments for suspensions and solutions, the pinning effect was supported for spherical colloidal suspensions on a cover glass. For anisotropically shaped particles, however, a broad ring at the outside edge disappeared and a round hill appeared instead. Furthermore, the pinning effect was not supported in a glass dish and a watch glass. It should be mentioned further that theoretical studies for the convectional patterns have been made mainly using the Navier–Stokes equations, but these are not always successful [13–18]. The main cause for this is undoubtedly due to the insufficient experimental studies so far. It should be noted further that the *size*, *shape*, *conformation*, and/or *flexibility* information of particles and/or solutes (molecules) is transformed cooperatively and further accompanied with the *amplification* and *selection* into the succeeding sedimentation and drying patterns in the course of dryness of solutions and suspensions.

Sedimentation dissipative patterns in the course of drying suspensions of colloidal silica spheres (183 nm to1.2 μm in diameter) [19–24, this work], size-fractionated bentonite particles [25], green tea (Ocha) [26], and Miso soup (Okubo, publication in preparation) have been studied in detail in a glass dish, a cover glass, a watch glass, and others, for the first time in our laboratory. The broad ring patterns were formed within several 10 min in suspension state by the convectional flow of water and the colloidal particles. It was clarified that the sedimentary particles were suspended above the substrate and always moved by the external force fields including convectional flow and sedimentation. The sharpness of the broad rings was sensitive to the change in the room temperature and/or humidity. The main cause for the broad ring formation is due to the convectional flow of water and colloidal particles at the different rates, where the rate of the latter is slower than that of the former. Quite recently, dynamic sedimentation patterns formed cooperatively from the distorted spoke-like convectional structures of colloidal particles were observed for coffee and black tea (Okubo, publication in preparation).

Drying dissipative patterns have been studied for suspensions and solutions of many kinds of colloidal particles [8, 9, 11, 19–42; this work; Okubo, publication in preparation], linear-type synthetic and bio-polyelectrolytes [43, 44], water-soluble neutral polymers [45, 46], ionic and non-ionic detergents [47–49], gels [50], and dyes [51] mainly on a cover glass. The macroscopic broad ring patterns of the hill accumulated with the solutes in the outside edges always formed. For the non-spherical particles, the round hill was formed in the center area in addition to the broad ring. Macroscopic spoke-like cracks or fine hills including flickering spoke-like ones were also observed for many solutes. Furthermore, fractal patterns such as branch-like, arc-like, block-like, star-like, cross-like, and string-like ones were observed in the microscopic scale. These microscopic drying patterns were reflected from the *shape*, *size*, and/or *flexibility* of the solutes themselves. Microscopic patterns also formed by the translational Brownian diffusion of the solutes and the electrostatic and/or the hydrophobic interactions between solutes and/or between the solutes and the substrate in the course of the solidification. One of the very important findings in our experiments is that the primitive vague patterns were formed already in the concentrated suspensions or solutions before dryness, and they grew toward fine structures in the process of solidification.

In this work, sedimentation and drying dissipative patterns of colloidal crystals of silica spheres (183 nm in diameter) have been studied in the macroscopic and microscopic scales. One of the main purposes of this work is clarification of the colloidal size effect on the dissipative patterns with the help of the experimental data of the colloidal silica spheres having different sphere sizes in a watch glass reported hitherto [19, 21, 22].

Experimental

Materials

CS161 silica spheres were kindly donated from Catalysts & Chemicals Ind. Co. (Tokyo). Diameter, standard deviation from the mean diameter, and the polydispersity index of the spheres were 183 nm, 18.6 nm, and 0.10, respectively. These size parameters were determined through an electron microscope (Hitachi, H8100) in Gifu University. The sample was treated on a mixed bed of cation- and anion-exchange resins [Bio-Rad, AG501-X8(D), 20–50 mesh] for 6 years before use, since newly produced silica spheres always released a considerable amount of alkali ions from the porous sphere surfaces for a long time. Water used for the sample purification and preparation was purified by a Milli-Q reagent grade system (Milli-RO5

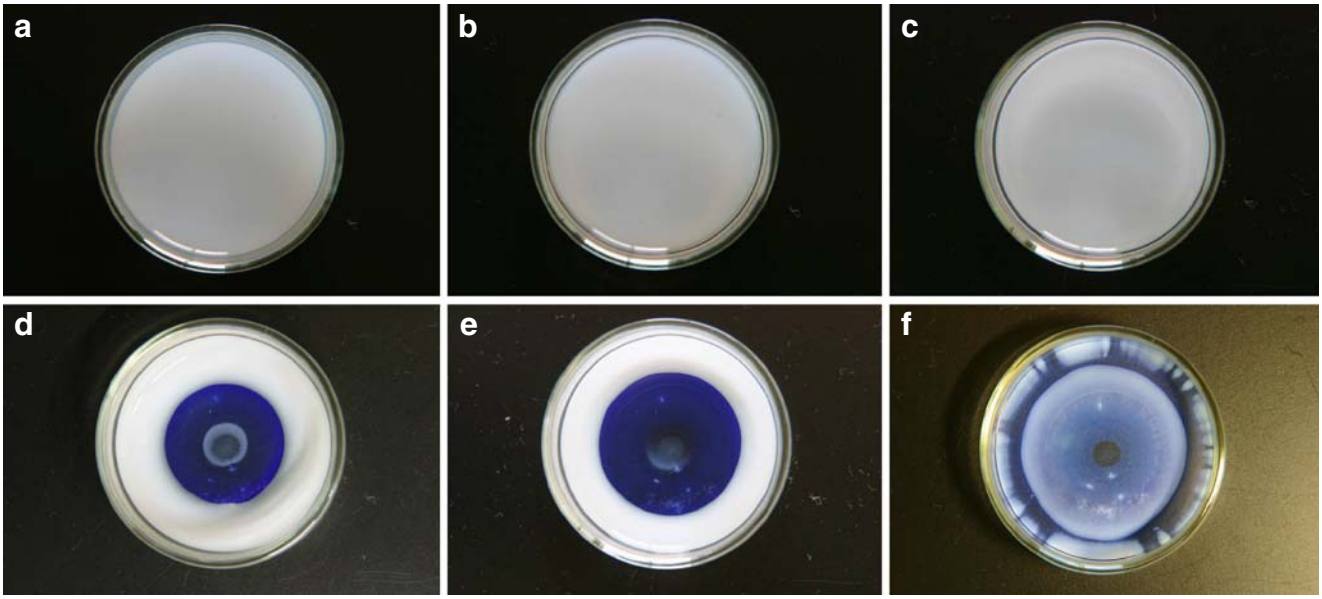

Fig. 1 Sedimentation and drying patterns of CS161 silica suspensions in a glass dish at 27 °C. ϕ=0.00215, 10 mL, code 286. **a** 30 min after setting, **b** 25 h, **c** 75 h, **d** 92.1 h, **e** 93.3 h, **f** 12.4 day, dry

plus and Milli-Q plus, Millipore, Bedford, MA, USA). Standard aqueous solution of sodium chloride at 0.1 mol/L (M) was purchased from Wako Chemicals Co. (Osaka).

Observation of the dissipative structures

Ten or 4 mL of the aqueous suspension of CS161 spheres was placed carefully and gently into a glass dish (42 mm in inner diameter and 15 mm in height, code 305-02, TOP Co. Tokyo) or a medium size watch glass (70 mm in diameter, TOP Co. Tokyo), respectively. The dish was flat without any disordered light reflection patterns as seen through the naked eyes. Observation of the sedimentation and drying patterns was made for the suspensions set on a desk until the suspensions were dried up completely in an air-conditioned room at 27 °C. The humidity of the room air of the laboratory was between 50% and 65%, which was not regulated. Concentrations of CS161 and NaCl ranged from 0.000086 to 0.0129 in volume fraction and from 0.0003 to 0.03 M, respectively.

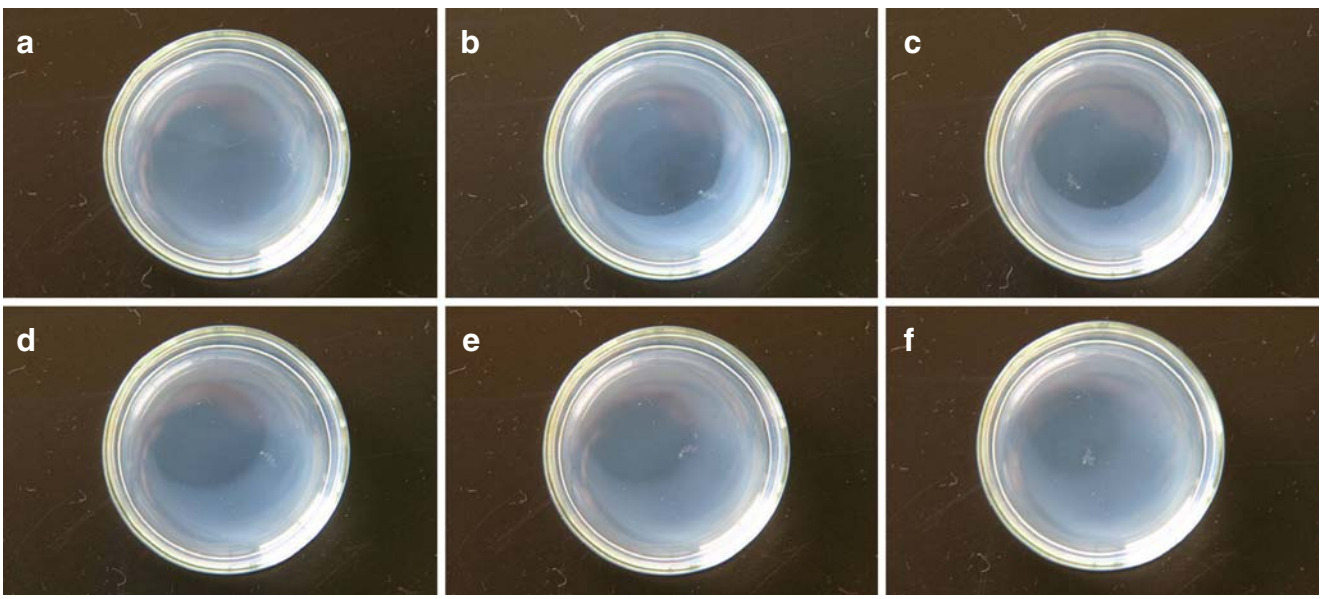

Fig. 2 Change in the sedimentation patterns of CS161 silica spheres in a glass dish 27 °C, 45 min after setting. ϕ=0.000086, 10 mL, code 281. **a** 0 min, 28.8 °C, 67%, air conditioner switched ON after taking pictures; **b** 20 min, 26.6 °C, 53%; **c** 40 min, 25.5 °C, 50%; OFF **d** 85 min, 26.5 °C, 63%; **e** 105 min, 27.7 °C, 66%; **f** 135 min, 28.9 °C, 67%

Macroscopic dissipative structures were observed on a Canon EOS 10D digital camera (Canon Co. Tokyo) with a lens (EF 28–200 mm, f=3.5–5.6 USM, Canon). Microscopic structures were observed with a metallurgical microscope (PME-3, Olympus Co., Tokyo).

Results and discussion

Sedimentation and drying patterns in a glass dish

Figure 1 shows the sedimentation (a to e) and drying patterns (f) of CS161 spheres when sphere concentration is 0.00215 in volume fraction. Coexistence of the sedimentation and drying patterns are observed in Fig. 1d,e. Clearly, broad ring patterns were observed at the outside area of the dish without cap in the suspension phase, and the suspensions dried up after 12.4 days. It should be recalled that the broad ring patterns did not appear in a dish with cap for colloidal silica spheres, 1.2 μm in diameter [20]. Ten milliliters of the aqueous suspensions of CS300 silica spheres (305 nm in diameter) at 0.00228 in volume fraction in a glass dish with a cap was dried up after 110 days at room temperature [21]. The same suspension without cap was dried up after 8.4 days [21]. In the suspension state with cap, they also exhibited broad ring patterns. These results show that the shielding effect of a glass dish with a

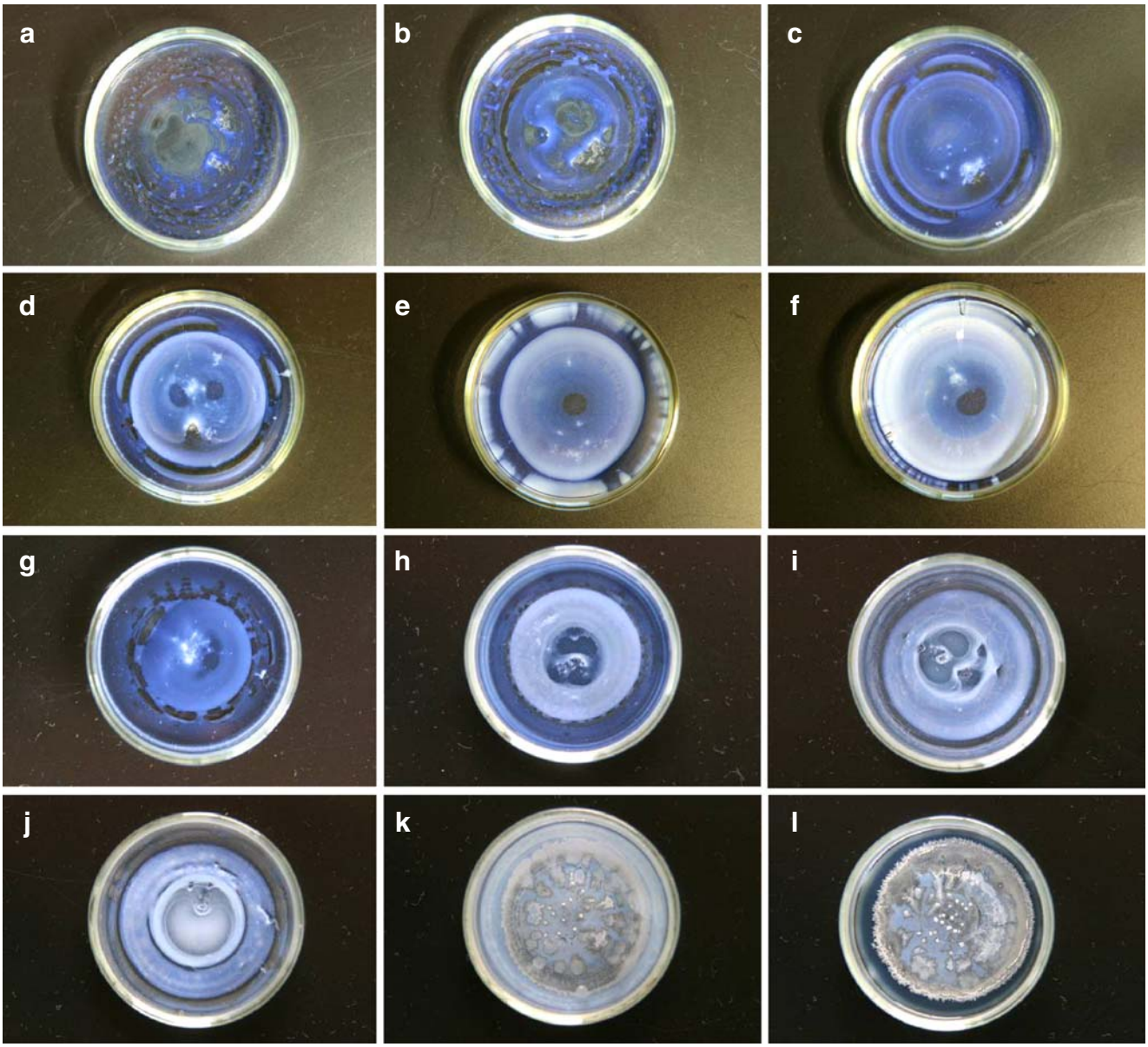

Fig. 3 Drying patterns of CS161 silica suspensions in a glass dish at 27 °C, 10 mL, after 12.4 day, dry. **a** ϕ=0.000086, **b** 0.000215, **c** 0.00043 M, **d** 0.00086, **e** 0.00215 M, **f** 0.013, **g** ϕ=0.00043, [NaCl]=0 M, **h** 0.0003 M, **i** 0.001 M, **j** 0.002 M, **k** 0.01 M, **l** 0.03 M

cap was not so complete for preventing the evaporation of water. However, evaporation and the resulted convectional flow were retarded efficiently with a cap. It should be noted that the broad rings formed rather quickly within 30–40 min after the suspension was set and even in the stage of the incomplete sedimentation of spheres, which shows that the convections of water and spheres are vigorous even at room temperature.

The main cause for the broad ring formation is due to the convectional flow of water and CS161 spheres in the different rates, where the rate of the latter is slower than that of the former under gravity. Especially, flow of the spheres from the center area toward the outside edges *in the lower layers* of the liquid, which was observed on a digital HD microscope directly from the movement of the very rarely occurring aggregates of the colloidal particles of Chinese black ink in a glass dish, is important [8]. Clearly, the convectional flow is enhanced by the evaporation of water at the liquid surface, which results to the lowering of the suspension temperature in the upper region of the suspension. When the colloidal spheres reach the edge wall of the dish at the outside region of the liquid, a part of the spheres will turn to upward and go back to the center region. However, many spheres may drop downward on the cell bottom close to the outside cell wall, where the effective horizontal flow of the spheres may stop temporarily and the accumulation of spheres proceeds accompanied with the evaporation of water by the capillary effect. This process must be followed by the broad ring accumulation of the spheres near the outside round edges.

It should be noted here that the formation of the broad ring patterns in the liquid phase reported here was observed first in a previous paper from the author's laboratory [20], which the author knew. However, the broad ring formation in the dried film has been observed so often for most of the solutions and suspensions examined by the researchers [27–32] and by our group [7–12, 19–26, 33–44, 46–51; Okubo, publication in preparation]. Recently, microgravity experiments were made for the observation of the drying dissipative patterns of deionized suspension of colloidal silica spheres [52]. Surprisingly, the broad ring patterns did not disappear even in microgravity. This supports strongly that both the gravitational and the Marangoni convections contribute to the broad ring formation on earth, and the latter is still important in microgravity.

We should note further that the broad ring patterns, which were generally observed for all the drying patterns of suspensions and solutions including the present paper, were formed already in the process of convectional flow of water and solutes in suspension state. The broad ring sedimentation structures have been observed also in a glass dish [22], in a polystyrene dish [20], in a watch glass [19, 21, 22], and even in a deep bowl [26] in our laboratory. It should be mentioned here that the dryness in a glass dish proceeded from the center area to the outer edge, and color changed clearly from whitey turbid in the liquid phase to the strongly iridescent blue colors in the solid phase. It should be noted here that the broad ring shown in Fig. 1f is observed at the inner area, not at the outside area of the dish, which will be discussed in detail below using Fig. 3.

Figure 2 shows the sedimentation patterns of the deionized suspensions of CS161 spheres, when the room temperature and the humidity changed by keeping switch of the compressor *on* or *off*. The experiments started 27 h and 45 min after the suspensions were set, where the stable sedimentation state was achieved. After picture a was taken at 28.8 °C and 67% in humidity, the switch of the compressor was kept on. After further 20 min and 40 min, pictures b and c were taken. At these times, the

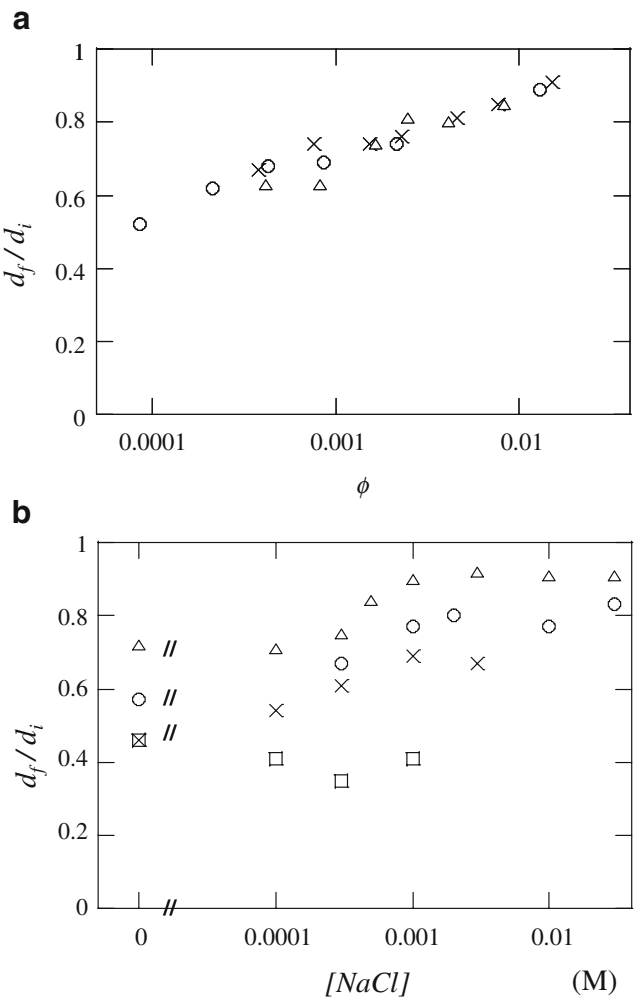

Fig. 4 **a** Plots of d_f/d_i of CS161 (*open circles*), CS300 (*crosses*), and CS550 (*open triangles*) in a glass dish as a function of ϕ. **b** Plots of d_f/d_i of the broad ring areas of sodium chloride for the suspensions of CS161 (*open circles*), CS300 (*crosses*), CS550 (*open triangles*), and the areas of CS300 spheres (*open squares*) as a function of [NaCl]. ϕ_{CS161}=0.00043, ϕ_{CS300}=0.00038, ϕ_{CS550}=0.00083

values of the room temperature and humidity decreased to 26.6 °C and 53% and 25.5 °C and 50%, and the sedimentation patterns became sharp with time. After taking picture c, the compressor was switched off. Now, the patterns became vague after 85, 105, and 135 min, respectively, where both the temperature and the humidity of the laboratory increased with time. The convectional flow of spheres and water should become fast, when the temperature and also the humidity above the air–suspension interface decrease. Thus, it is supported that the convectional flow of spheres and water is the main cause for the broad ring sedimentation pattern. It should be noted here that the slopes, not the absolute values, of the temperature and/or humidity with time are important for the rates of the convectional flows. Changes in the sharpness of the broad rings responding to the room temperature and humidity were also observed for other silica spheres having different diameters in a glass dish [21, 22].

Figure 3a–f shows the macroscopic drying patterns of CS161 spheres in a glass dish at the initial sphere concentrations ranging from 0.000086 to 0.013 in volume fraction 12.4 days after the suspensions were set. The broad rings formed at the outside area of the dried film, but within the inner wall of the glass dish. The size of the

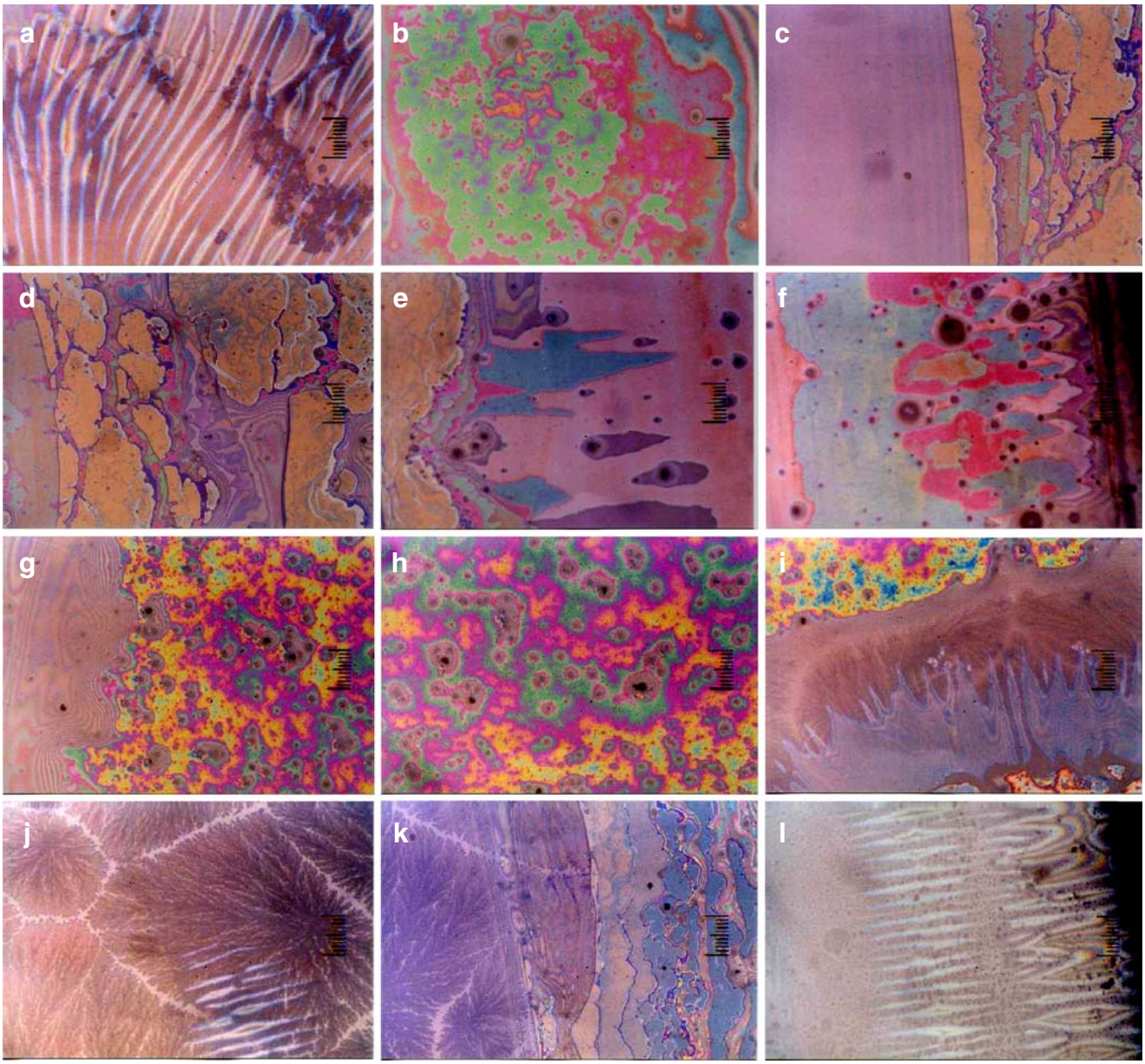

Fig. 5 Drying patterns of CS161 silica spheres in a glass dish at 27 °C. ϕ=0.000429, [NaCl]=0 M, 10 mL, dry, code 291, from center (**a**) to right edge (**f**), [NaCl]=0.0003 M, 10 mL, dry, code 292, from center (**g**) to right edge (**l**)

broad ring increased as the initial sphere concentration increased as clearly shown in the figures. All the dried films were bluish with the iridescent Bragg diffraction of light by the crystal-like array of the colloidal spheres in the film. The ratio of the size of the broad ring in diameter against that of the inner diameter of the glass dish, d_f/d_i, was plotted as a function of the initial sphere concentration, ϕ in Fig. 4a for all the drying patterns of silica spheres of different sizes examined hitherto. Interestingly, the d_f/d_i values increased linearly as the logarithms of sphere concentration, log ϕ, and further located on the same line irrespective of sphere sizes in the range of 183 nm to 1.2 μm within the experimental errors. These results show that the size of the broad ring in a glass dish is sensitive to the sphere concentration but not so much to the sphere size. Figure 3c–f also shows that the spoke-like fine cracks appeared especially in the areas of the broad rings. Interestingly, the wave-shaped structures formed in the areas between the outside edges of the film and the inner wall of the glass dish, when sphere concentration is lower than 0.000215 (see Fig. 3a,b). It should be mentioned here that the drying frontier started at the center of the glass dish and moved toward the outer cell wall with time. This direction of the drying frontier movement was just opposite to that on a cover glass, where the frontier moved from the outside edges of the suspension to the center.

Figure 3g–l shows the macroscopic drying patterns of CS161 suspensions with the coexistence of NaCl and in their absence at the dried state, 12.4 days after suspensions were set. Distinct differences were not observed among the broad ring patterns in the suspension state containing different amounts of sodium chloride, though the pictures showing these were omitted in this paper. However, it looks that the broad rings of the sedimentation pattern were slightly sharp for the salt-containing suspensions as seen through the naked eyes. The electrical double layers around the spheres are thin when the ionic concentration is high. Thus, the translational diffusion of the spheres will be much vigorous, since the effective size of spheres including the double layers decreases. Macroscopic drying broad ring patterns were observed clearly for all the samples, and the size of the broad ring increased as the salt concentration increased as clearly shown in the figure. Surprisingly, quite different macroscopic patterns appeared for the suspensions containing sodium chloride higher than 0.01 M. Furthermore, the cooperative microscopic structures were also observed for CS161 spheres as observed for CS1000A [20], CS300 [21], and CS560 spheres [22], which will be described in detail below using the microscopic pictures shown in Fig. 5.

It should be mentioned here that the colors of the dried films changed greatly and systematically from bluish to greenish or pinky, pinky or whitey, and whitey as spheres changed from CS161 (183 nm in diameter) to CS300 (305 nm), CS550 (560 nm), and CS1000A (1.205 μm), respectively. These colors are mainly from the Bragg diffraction of light by the crystal-like arrays of spheres. The primary peak wavelength (λ_p) in the reflection spectroscopy of colloidal crystals at the scattering angle of 90° is estimated from the nearest-neighbored intersphere distance (D) of the face-centered and/or body-centered cubic lattices.

$$\lambda_p = nD/0.6124 \quad (1)$$

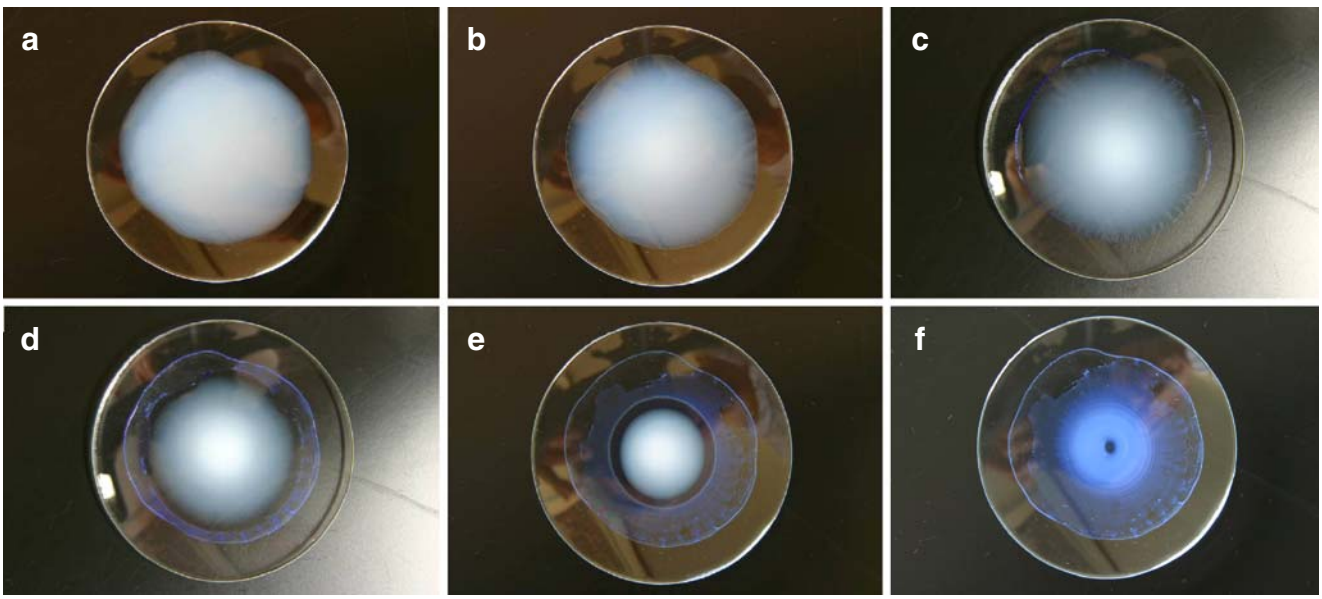

Fig. 6 Convectional, sedimentation, and drying patterns of CS161 silica suspensions in a watch glass at 27 °C. ϕ=0.00107, 4 mL, code 303. **a** 20 min after setting, **b** 2.9 h, **c** 6.8 h, **d** 12.7 h, **e** 18.7 h, **f** 22.7 h, dry

Here, the refractive indices of the liquid and dried film (n) are given in Eq. 2.

$$n = \phi \times [\text{refractive index of silica sphere}] + (1 - \phi) \times [\text{refractive index of air}] \quad (2)$$

Refractive indices of silica and air were assumed to be 1.5 and 1.00, respectively. For the dried film, ϕ and D are estimated to be 0.74 and the diameter of spheres, respectively. Here, the spheres in the dried film were assumed to be attached to each other and distribute in the closed-packed colloidal crystal structure. The λ_p values of the dried films are estimated to be 420 nm, 700 nm, 1.3 μm, and 2.8 μm for CS161, CS300, CS550, and CS1000A spheres, respectively. Depending on the scattering angles, the color should change, but the color is estimated roughly to be blue, green, red, and ultra-red (actually purely white by the very strong multiple scattering), respectively.

Figure 4b shows the ratio of the final size of dried broad ring pattern against the inner size of the glass dish, d_f/d_i for the sphere–NaCl mixtures. Clearly, the d_f/d_i values increased as the concentration of the salt increased for CS161 + NaCl (denoted by open circles), CS300 + NaCl (crosses), and CS550 + NaCl mixtures (open triangles). For CS300 + NaCl systems [21], another broad ring appeared clearly in the inner area of the outward broad ring as shown by open squares in Fig. 4b. For CS161 + NaCl and CS550 +

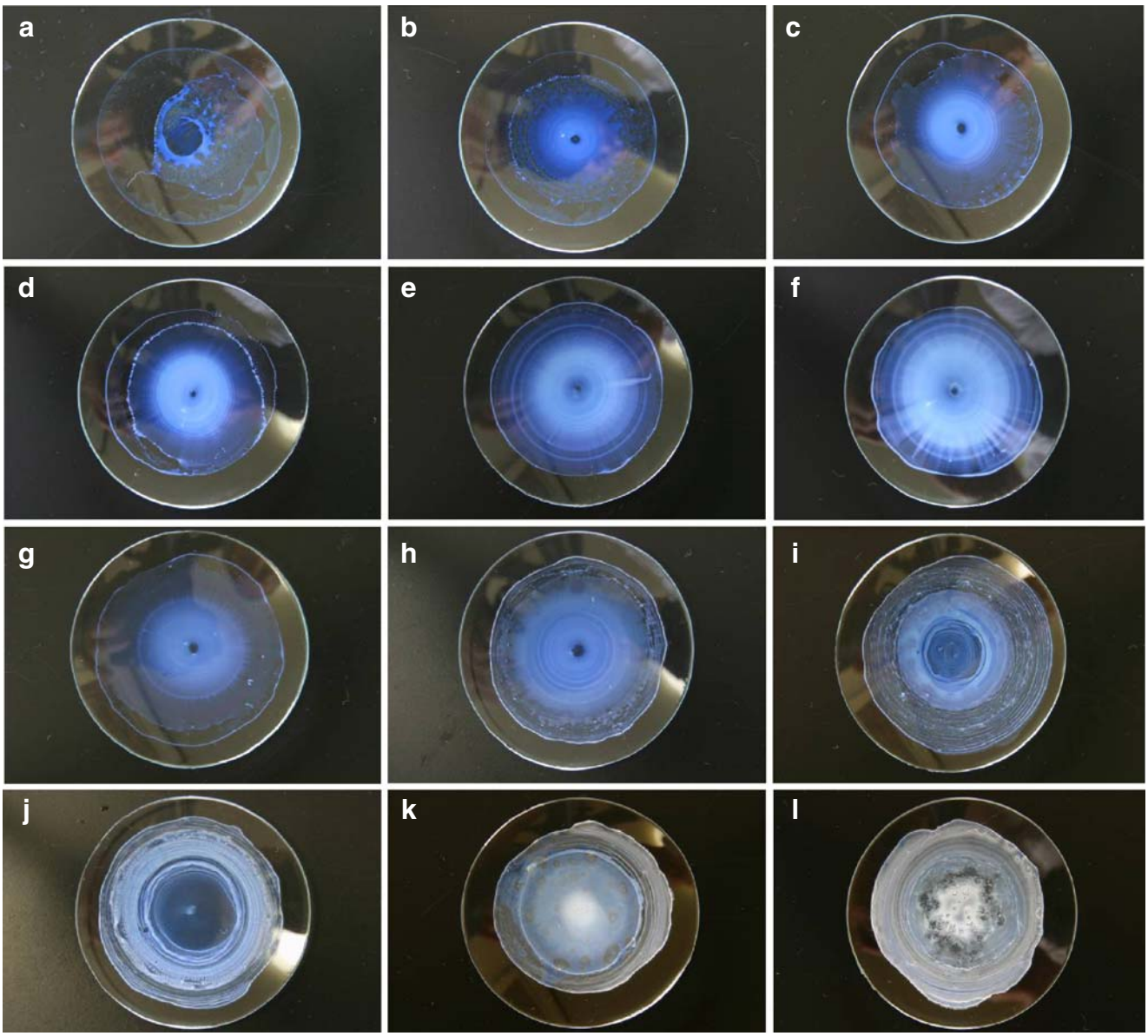

Fig. 7 Drying patterns of CS161 silica suspensions in a watch glass at 27 °C, 4 mL. **a** ϕ=0.000215, **b** 0.000429, **c** 0.00107 M, **d** 0.00215, **e** 0.00322 M, **f** 0.00429, **g** ϕ=0.00107, [NaCl]=0 M, **h** 0.00075 M, **i** 0.0025 M, **j** 0.0075 M, **k** 0.025 M, **l** 0.075 M

NaCl mixtures, the patterns of the inner broad rings were also observed but not so clear for quantitative analysis. The inner broad rings disappeared for CS1000A + NaCl mixtures. It is highly plausible from previous work of binary and ternary colloidal mixtures [23, 24] that the outward and inward broad rings in a glass dish are composed of mainly colloidal spheres and sodium chloride, respectively. In other words, the smaller solutes are segregated to the outer regions. This size effect is, however, not so effective in a glass dish compared with the effect in a watch glass. These features are discussed below using Fig. 8a,b in detail.

Figure 5 shows a typical example of the microscopic patterns of the dried film observed in Fig. 3, where the extended pictures were taken from the center to the right edge. Colorful microstructures were observed. These iridescent colors are due to the Bragg diffraction of light by the crystal array of the colloidal spheres in the dried film. It should be mentioned further that the main cause of the microstructures will be the traces of the convectional flow of spheres and water molecules on a glass dish. It should be mentioned here that the beautiful characteristic patterns of the colloidal spheres and sodium chloride mixtures were observed in Fig. 5j–l. Here, whitey parallel line areas are composed of sodium chloride. These observations demonstrate that the cooperative interactions between silica spheres and sodium chloride play an important role for the pattern formation in the processes of the solidification. Similar cooperative patterns were also observed for other salt mixtures of silica spheres having different sizes in a glass dish [20–22].

Convectional, sedimentation, and drying patterns in a watch glass

Figure 6 shows one of the typical examples of the sedimentation and drying patterns in the course of dryness of aqueous suspensions of CS161 spheres on a watch glass. Interestingly, spoke-like convectional patterns were observed for the first time in aqueous suspensions of colloidal silica spheres in this work (see Fig. 6c). When the colloidal suspension of CS161 spheres was kept still in a watch glass, sedimentation of the spheres took place within 3 h especially at the upper layers of the suspension, and a broad hill was observed first and then a broad ring pattern appeared at the central area of the watch glass as seen through the naked eyes (see Fig. 6b–e). The suspensions dried up after 22.7 h as shown in Fig. 6f. The main causes for the broad ring formation are again the convectional flow of water and CS161 spheres in the different rates and due to the evaporation of water from the outer edges. The flow of spheres from the center area toward the outside edges in the lower layer of the liquid is especially important (Okubo, publication in preparation). Enhancement of the convectional flow by the evaporation of water must be followed by the broad ring accumulation of the spheres near the outside round edges. It should be noted here that the sphere accumulation at the deepest point of a watch glass did not take place in the dried film.

Figure 7 shows the drying patterns of CS161 suspensions at different sphere concentrations from 0.000215 to 0.00429 in volume fraction (a to f) and with sodium chloride (g–l). These pictures, especially without salt, show clearly that the sphere accumulation at the deepest central point did not take place compared with the upper whitey and bluish broad ring area. The main cause for the broad ring formation is again the convectional flow of water and CS161 spheres at the different rates. Flow of spheres from the central area toward the outside edges in the lower layer of the liquid is very important [8]. Enhancement of the

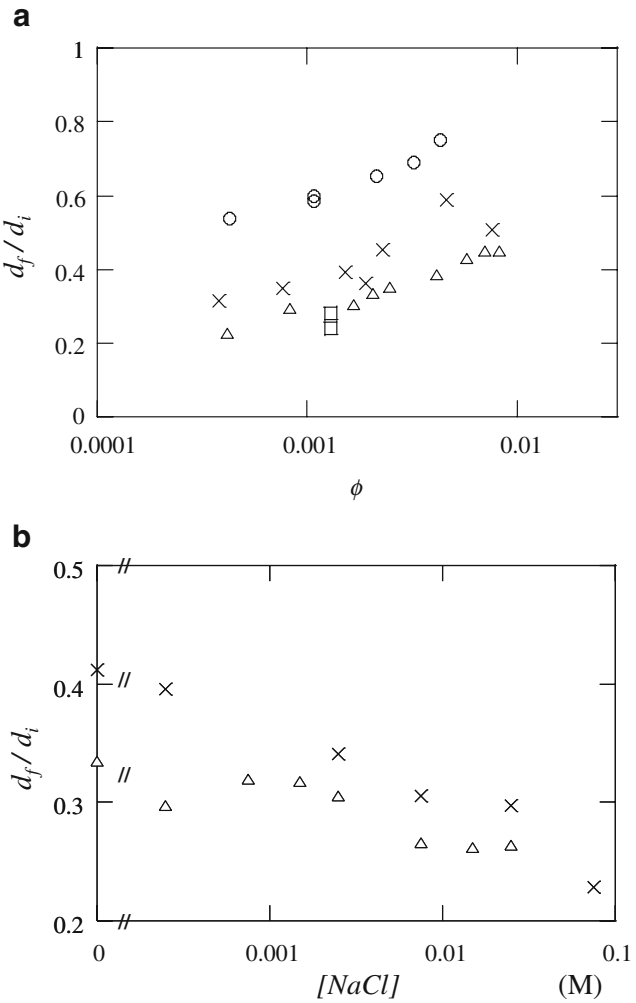

Fig. 8 **a** Plots of d_f/d_i of CS161 (*open circles*), CS300 (*crosses*), CS550 (*open triangles*), and CS1000A (*open squares*) in a watch glass as a function of ϕ. **b** Plots of d_f/d_i of CS300 (*crosses*), CS550 (*open triangles*) in a watch glass as a function of [NaCl]. ϕ_{CS300}= 0.0019, ϕ_{CS550}=0.00207

convectional flow by the evaporation of water must be followed by the broad ring accumulation of the spheres near the outside edges.

We should note here that all the sedimentary spheres in the sedimentation spheres float above the watch glass cell surface by the repulsive interaction between the cell and spheres intermediated with the electrical double layers formed from the cell surface and spheres. It should be further mentioned that the size of the broad ring in a watch glass clearly increased drying through visual observations as sphere concentration increased (see Fig. 7a–f). Furthermore, the size of the broad rings on a watch glass appears to decrease as sphere size increases, when the observations of the drying patterns are compared among the examined colloidal silica spheres of 183 nm (this work), 305 nm [21], 560 nm [22], and 1.2 μm in diameter [19]. In Fig. 8a, the ratios of the final size of the broad rings against the initial size of the liquid, d_f/d_i, of CS161, CS300, CS550, and CS1000A on a watch glass are plotted against the sphere concentrations. Clearly, d_f/d_i values increased as sphere concentration increased and/or sphere size decreased. This is due to the fact that the sedimentary spheres locate at the positions in balance between the flow toward the outside (or upward) direction by the convection and the inside flow by the sedimentary forces on a watch glass. Then, the convectional flow of small spheres should be much stronger. The main contribution of the outward (or upward) flow of spheres is the translational diffusion forces of the colloidal spheres, then, d_f/d_i should be proportional to the inverse sphere size from the Stokes–Einstein equation (Eq. 3).

$$D_t = k_B T/3\pi\eta d \tag{3}$$

Here, D_t is the translational diffusion coefficient, d is the diameter of colloidal spheres, η is the viscosity of water, k_B is the Boltzmann constant, and T is the absolute temperature. The electrical double layers move with the colloidal spheres, though the double layers are distorted substantially. d values can be replaced with the effective diameter of spheres, d_{eff}, given in Eq. 4.

$$d \cong d_{eff} = d_o + 2 \times D_l \tag{4}$$

$$D_l = \left(4\pi e^2 n/\varepsilon k_B T\right)^{-1/2} \tag{5}$$

d_o is the real diameter of the sphere and D_l is the Debye screening length given in Eq. 5, where e is the electronic charge, ε is the dielectric constant of water, and n is the concentration of free state cations and anions in suspension, given by $n=n_c+n_s+n_o$. n_c is the concentration (number of ions per cubic centimeter) of diffusible counter-ions, n_s is the concentration of foreign salt, sodium chloride in this

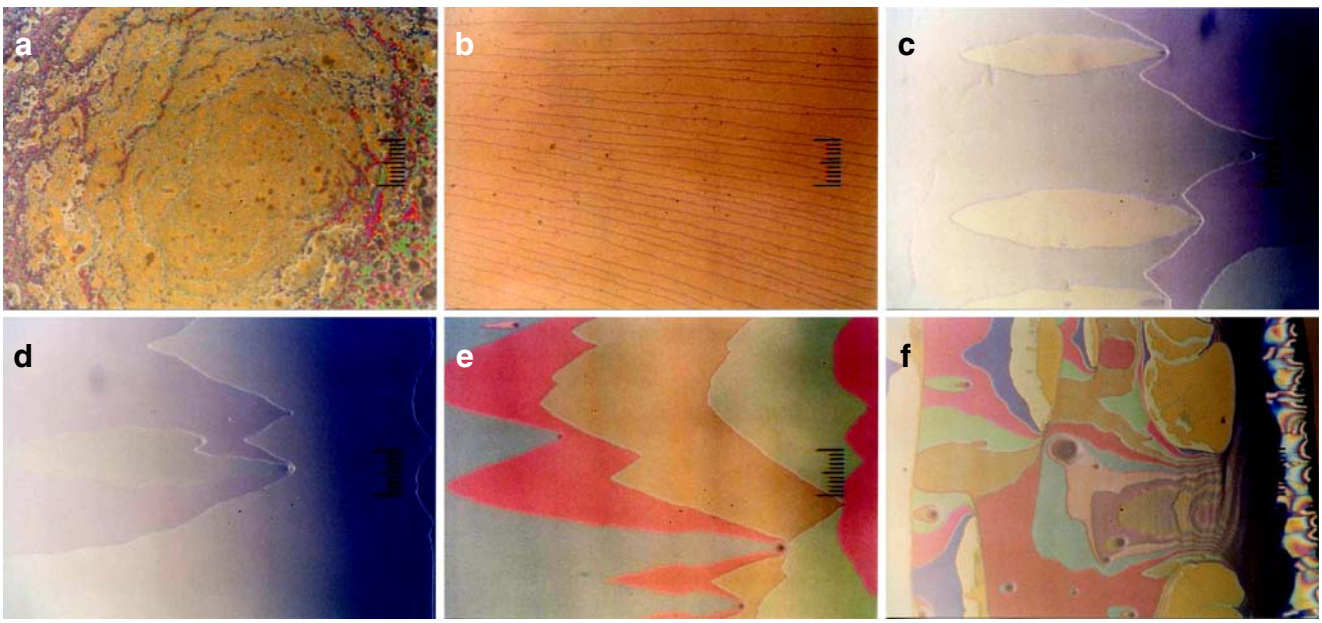

Fig. 9 **a** Microscopic drying patterns of CS161 silica suspensions in a watch glass at 27 °C. ϕ=0.00107, 4 mL, code 311, from center (**a**) to right edge (**f**), full scale=0.2 mm. **b** Microscopic drying patterns of CS161 silica suspensions in a watch glass at 27 °C. ϕ=0.00107, **a** to **f**: [NaCl]=0.0025 M, 10 mL, code 313, from center (**a**) to right edge (**f**), **g** to **l**: [NaCl]=0.0075 M, code 316, from center (**g**) to right edge (**l**), full scale=0.2 mm

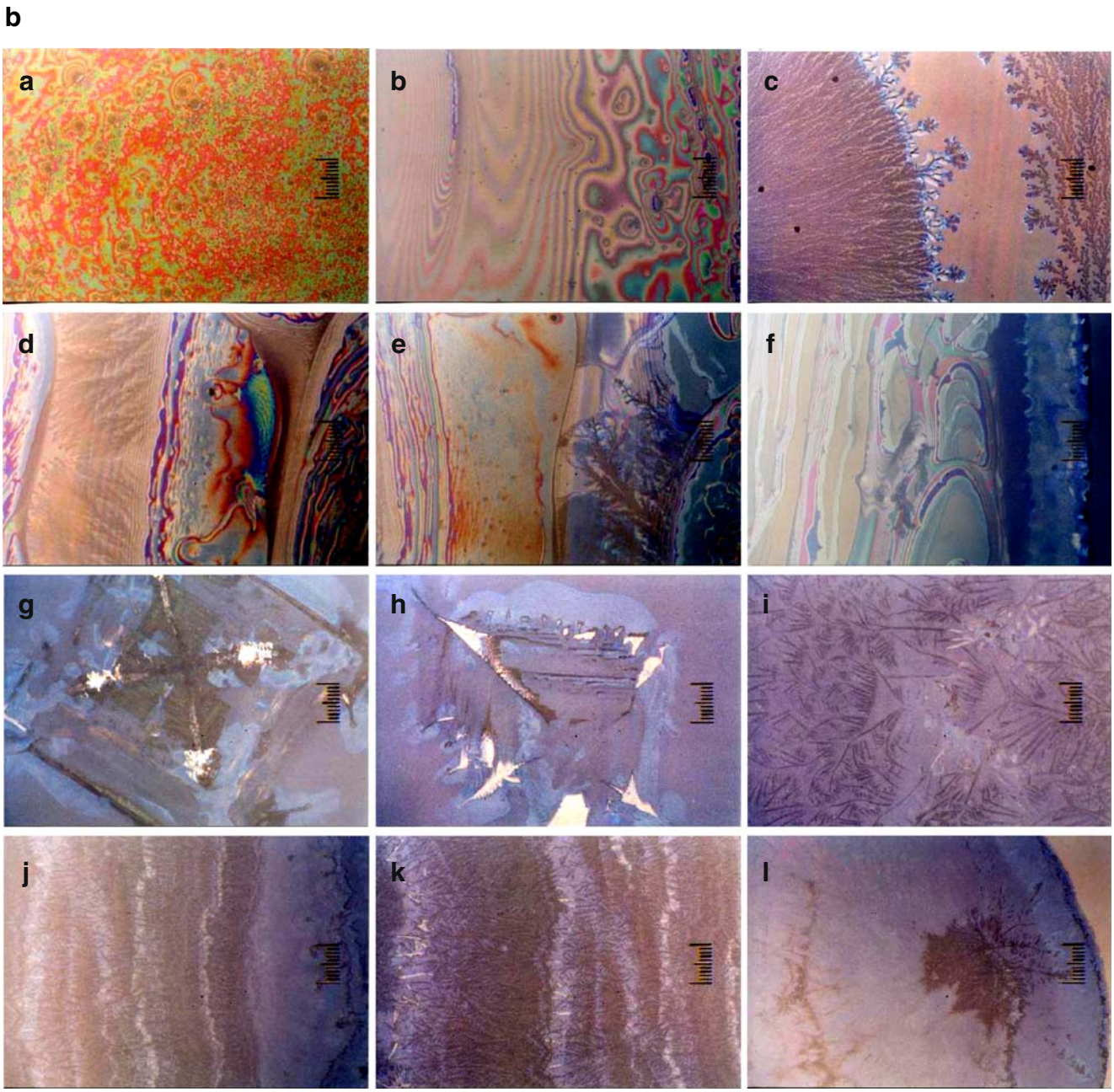

Fig. 9 (continued)

work, and n_o is the concentration of both H^+ and OH^- from the dissociation of water. On the other hand, the inward (or downward) flow of spheres will be given by the sedimentation of spheres. The sedimentation coefficient, S is given in Eq. 6 [53].

$$S = (\rho - \rho_o) \sin\theta g d_0^3 / 18\eta d_{\text{eff}} \quad (6)$$

Here, θ is the slope angle of the cell surface, which is 0° at the center and increases at the outward positions. ρ and ρ_o are the specific gravities of the suspension and water, respectively, and g is the gravitational constant. Further discussion on the broad ring size using Eqs. 3 and 6 is quite difficult at present. However, size dependency observed experimentally of the broad rings on the colloidal size is explained further qualitatively by comparing Eqs. 3 and 6, which are the outward and inner forces of the spheres, respectively. The outward forces increase as sphere size decreases, since D_t is proportional to the inverse size of the colloidal sphere. The inward forces also increase as sphere size increases, since S is proportionally increased as d_o^3/d_{eff} increases. It should be mentioned here that the

main cause for the increase of the broad ring size with increasing sphere concentration is the increase of the number of spheres accumulated in the cell, in which spheres have their own excluded volumes. In conclusion, Fig. 8a shows clearly that the size of the broad ring in a watch glass increases systematically as sphere size decreases. This result is quite consistent with the facts that the size segregation and the semi-quantitative analyses of the binary and ternary mixtures of colloidal silica spheres having different sizes were made successfully from their drying patterns [23, 24].

The salt effect on the d_f/d_i values on a watch glass is shown in Fig. 8b. The main cause for the decrease of d_f/d_i with the salt concentration will be the fact that sodium chloride ions are very small compared with the colloidal spheres and segregated substantially toward the outward region of the cell. However, it is highly plausible that the segregation effect is not so effective and a part of the colloidal spheres also locates at the outward positions accompanied with the salt because the outward convectional flow of spheres and salts resulted from the integration of the huge number of small circulating cell convections such as Terada cells and Bernard cells described in the "Introduction" section. The other important cause for the decrease in d_f/d_i values with salt addition is the thinning of the electrical double layers which resulted to the decrease of the effective size of colloidal spheres including the electrical double layers formed around colloidal spheres, d_{eff} (see Eq. 5).

Figure 9 shows the microscopic pictures of the drying patterns of CS161 suspensions at φ=0.00107 from the central area (a) to the right-hand side edge (f). Three different types of patterns appeared from the central area to the outside edge regions: (1) circular oriented grain-like patterns in the central area (see Fig. 9a), (2) spoke-like patterns in the radial direction (b), and (3) very colorful patched block-like patterns (c to f). It should be noted that the multi-strings circle-like patterns, which were so often observed for larger spheres (CS300, CS550, and CS1000A spheres [19, 21, 22]) were not observed for CS161 spheres in a watch glass. These three types of the microstructures support the existence of the three different modes in the convectional flows of water and solutes as a function of the distance from the center of the watch glass, though the explanation of the reason why these patterns appeared is quite difficult at present. It should be noted again that the iridescent and colored pictures are due to the Bragg diffraction of light by the crystal array of CS161 spheres in the dried film.

Acknowledgments Financial support from the Ministry of Education, Culture, Sports, Science and Technology, Japan and the Japan Society for the Promotion of Science is greatly acknowledged for Grants-in-Aid for Exploratory Research (17655046) and Scientific Research (B) (18350057), respectively. Catalysts and Chemicals Co. is thanked deeply for providing the colloidal silica sphere samples used in this work. Professor Akira Tsuchida of Gifu University is acknowledged greatly for his kind support of the author's experiments and useful discussion on dissipative patterns.

References

1. Gribbin G (1999) Almost everyone's guide to science. The universe, life and everything. Yale University Press, New Haven
2. Ball P (1999) The self-made tapestry. Pattern formation in nature. Oxford University Press, Oxford
3. Okubo T (2001) Beautiful world of colloids and interfaces (Japanese). Matsuo, Gifu
4. Terada T, Yamamoto R, Watanabe T (1934) Sci Pap Inst Phys Chem Res Jpn 27:173 Proc Imper Acad Tokyo 10:10
5. Terada T, Yamamoto R, Watanabe T (1934) Sci Pap Inst Phys Chem Res Jpn 27:75
6. Terada T, Yamamoto R (1935) Proc Imper Acad Tokyo 11:214
7. Nakaya U (1947) Memoirs of Torahiko Terada (Japanese). Kobunsya, Tokyo
8. Okubo T, Kimura H, Kimura T, Hayakawa F, Shibata T, Kimura K (2005) Colloid Polym Sci 283:1
9. Okubo T (2006) Colloid Polym Sci 285:225
10. Deegan RD, Bakajin O, Dupont TF, Huber G, Nagel SR, Witten TA (1997) Nature 389:827
11. Okubo T, Okamoto J, Tsuchida A (2008) Colloid Polym Sci 286:1123
12. Okubo T, (2008) Colloid Polym Sci 286:1307
13. Palmer HJ (1976) J Fluid Mech 75:487
14. Anderson DM, Davis SH (1995) Phys Fluids 7:248
15. Pouth AF, Russel WB (1998) AIChEJ 44:2088
16. Burelbach JP, Bankoff SG (1998) J Fluid Mech 195:463
17. Deegan RD, Bakajin O, Dupont TF, Huber G, Nagel SR, Witten TA (2000) Phys Rev E 62:756
18. Fischer BJ (2002) Langmuir 18:60
19. Okubo T (2006) Colloid Polym Sci 284:1191
20. Okubo T (2006) Colloid Polym Sci 284:1395
21. Okubo T, Okamoto J, Tsuchida A (2007) Colloid Polym Sci 285:967
22. Okubo T (2007) Colloid Polym Sci 285:1495
23. Okubo T, Okamoto J, Tsuchida A (2008) Colloid Polym Sci 286:385
24. Okubo T, Okamoto J, Tsuchida A (2008) Colloid Polym Sci 286:941
25. Yamaguchi T, Kimura K, Tsuchida A, Okubo T, Matsumoto M (2005) Colloid Polym Sci 283:1123
26. Okubo T (2006) Colloid Polym Sci 285:331
27. Vanderhoff JW (1973) J Polym Sci Symp 41:155
28. Nicolis G, Prigogine I (1977) Self-organization in non-equilibrium systems. Wiley, New York
29. Ohara PC, Heath JR, Gelbart WM (1997) Angew Chem 109:1120
30. Maenosono S, Dushkin CD, Saita S, Yamaguchi Y (1999) Langmuir 15:957
31. Nikoobakht B, Wang ZL, El-Sayed MA (2000) J Phys Chem 104:8635
32. Ung T, Litz-Marzan LM, Mulvaney P (2001) J Phys Chem B 105:3441
33. Okubo T, Okuda S, Kimura H (2002) Colloid Polym Sci 280:454
34. Okubo T, Kimura K, Kimura H (2002) Colloid Polym Sci 280:1001
35. Okubo T, Kanayama S, Kimura K (2004) Colloid Polym Sci 282:486

36. Okubo T, Yamada T, Kimura K, Tsuchida A (2005) Colloid Polym Sci 283:1007
37. Okubo T (2006) Molecular and colloidal electro-optics, Stoylov SP, Stoimenova MV (eds), 573, Taylor & Francis
38. Okubo T, Nozawa M, Tsuchida A (2007) Colloid Polym Sci 285:827
39. Okubo T, Kimura K, Tsuchida A (2007) Colloids Surf B Biointerfaces 56:201
40. Okubo T, Nakagawa N, Tsuchida A (2007) Colloid Polym Sci 285:1247
41. Okubo T (2008) Nanoparticles: syntheses, stabilization, passivation and functionalization. Nagarajan R, Hatton TA (eds), chap 19, ACS Book Washington DC
42. Okubo T, Kimura K, Tsuchida A (2008) Colloid Polym Sci 286:621
43. Okubo T, Kanayama S, Ogawa H, Hibino M, Kimura K (2004) Colloid Polym Sci 282:230
44. Okubo T, Onoshima D, Tsuchida A (2007) 285:999
45. Shimomura M, Sawadaishi T (2001) Curr Opin Colloid Interface Sci 6:11
46. Okubo T, Yamada T, Kimura K, Tsuchida A (2006) Colloid Polym Sci 284:396
47. Okubo T, Kanayama S, Kimura K (2004) Colloid Polym Sci 282:486
48. Kimura K, Kanayama S, Tsuchida A, Okubo T (2005) Colloid Polym Sci 283:898
49. Okubo T, Shinoda C, Kimura K, Tsuchida A (2005) Langmuir 21:9889
50. Okubo T, Itoh E, Tsuchida A, Kokufuta E (2006) Colloid Polym Sci 285:339
51. Okubo T, Yokota N, Tsuchida A (2007) Colloid Polym Sci 285:1257
52. Tsuchida A, Okubo T (2003) J Fiber Soc Jpn 59:264
53. Okubo T (1994) J Phys Chem 98:1472